

# Toward an Understanding of the Role of Water-Soluble Oligomers in the Emulsion Polymerization of Styrene–Butadiene–Acrylic Acid. Separation and Characterization of the Water-Soluble Oligomers

Xue-yi Yuan, Victoria L. Dimonie, E. David Sudol, and Mohamed S. El-Aasser\*

*Emulsion Polymers Institute, Center for Polymer Science and Engineering, Departments of Chemical Engineering and Chemistry, Lehigh University, 111 Research Drive, Bethlehem, Pennsylvania 18015*

*Received January 9, 2002; Revised Manuscript Received July 15, 2002*

**ABSTRACT:** A series of techniques were developed to quantitatively characterize the free water-soluble oligomers found in the aqueous phase in a model styrene/butadiene/acrylic acid (St/Bu/AA) batch emulsion terpolymerization process. Particular attention was paid to the early stages of the polymerization. Ultracentrifugation was used to accomplish the separation of the aqueous phase from the particle phase.  $^1\text{H}$  NMR, aqueous phase GPC, and GC techniques were used to determine the oligomer concentration as well as their composition and the surfactant concentration in the aqueous phase, the oligomer molecular weight, and the acrylic acid monomer conversion, respectively. The results were related to the overall conversion and the number of particles as a function of conversion. The oligomer concentration vs conversion curves for the model system show a maximum at around 12% conversion. However, the position of this maximum with respect to conversion is related to the surfactant concentration. The sharp decrease in the oligomer concentration after micelles disappeared, and the decrease in the number of particles was considered to have resulted from a strong interaction of these oligomers, which are rich in St and Bu units, with the polymer of the latex particle surface. Increasing the AA concentration in the recipe increased the water-soluble oligomer concentration and the number of particles, thereby increasing the rate of polymerization.

## Introduction

Water-soluble carboxylic acid monomers, such as acrylic acid (AA), methacrylic acid, and itaconic acid, are widely used in emulsion polymerization for the production of latexes used for paper coatings, textile coatings, and adhesives. The incorporation of the carboxyl groups on the latex particle surface, even in small amounts, provides many advantages, such as enhanced colloidal stability and adhesion to various substrates. Conventional emulsion polymer systems often use monomers that are relatively water-insoluble, such as styrene and butadiene. The primary reaction locus is inside the polymer particles, and aqueous-phase polymerization is usually considered to be negligible. Many industrial reaction systems, however, employ one or more monomers that have a significant water solubility. The concentration and extent of reaction of these water-soluble monomers in the aqueous phase may be significant, and conventional emulsion polymerization kinetics do not readily apply to these systems. Carboxylated latexes comprise an important class of industrial emulsion polymer systems involving water-soluble monomers. Carboxylic acid monomers (such as acrylic acid) are often completely soluble in water. However, they will still partition to varying extents into the organic phase depending on their relative hydrophobicity. In this case, significant amounts may exist in both the organic and aqueous phases.

Although the conversion of monomer to polymer in conventional emulsion polymerization systems is believed to take place primarily in the monomer swollen polymer particles, the oligomeric radicals formed in the water phase can play an important part in particle

nucleation and stabilization and in the characteristics of the final latex products. Most of the reported studies in the literature for emulsion polymerization systems involving carboxylic acids have focused on the overall kinetic scheme in order to predict reaction rates, copolymer composition, particle concentrations, and particle size. Most studies of water-phase oligomers have been concerned with only one or two monomers, because of the heterogeneous and complex nature of emulsion polymerization systems. Theoretical predictions for systems involving more than one monomer, especially terpolymer systems, are extremely difficult due to the extent of uncertainty of parameters needed for the modeling. Therefore, experimental determination of the aqueous phase species will be very important in providing a better understanding of the emulsion polymerization process in these systems, which will lead to better control of the final latex characteristics in various applications.

A model industrial emulsion polymerization system containing styrene (St), butadiene (Bu), and acrylic acid (AA) monomers is being investigated in this research. The goal is to investigate experimentally the formation of water-soluble oligomers during the emulsion polymerization and determine their relevance to the kinetics and mechanism of particle nucleation and growth.

## Experimental Section

**Materials.** Acrylic acid (AA) monomer ( $\text{CH}_2=\text{CHCOOH}$ , MW = 72.06 g/mol, 99% active) inhibited with 200 ppm of 4-methylhydroquinone (MHQ) (Aldrich) was distilled under vacuum at  $\sim 10$  mmHg and  $39^\circ\text{C}$  vapor temperature to remove the inhibitor. The purified acrylic acid was stored at  $\sim 14^\circ\text{C}$  under running tap water. Storage at a lower temperature ( $< 13^\circ\text{C}$ ) will freeze the liquid. Localized overheating or UV light may lead to violent autopolymerization.<sup>1</sup> The styrene (St) monomer ( $\text{CH}_2=\text{CHC}_6\text{H}_5$ ) was inhibited with 55 ppm of *p*-tert-

\* Corresponding author. E-mail mse0@lehigh.edu.

**Table 1. Model Recipe Used for the Synthesis of St/Bu/AA Latex<sup>a</sup>**

component	amount (g)
distilled–deionized water	21.66
sodium lauryl sulfate (SLS)	0.22
styrene (St)	5.22
butadiene (Bu)	3.90
acrylic acid (AA)	0.38
potassium persulfate	0.019 <sup>b</sup>

<sup>a</sup> Monomers (mol %): Bu/St/AA = 57/39/4. Total solids (wt %) = 30. Oil/water ratio (wt) = 1/2.4. [SLS] = 32 mM (cmc = 9 mM in pure water at 70 °C). <sup>b</sup> [I] = 3.17 mM, based on water.

butylcatechol (Aldrich), which was removed by passing the mixture through a bed of activated aluminum oxide (Brockmann I Standard grade, basic, ~150 mesh, 58 Å, 155 m<sup>2</sup>/g surface area, Aldrich). The purified styrene monomer was stored in a refrigerator at about –2 °C until use. Gaseous butadiene (Bu) monomer (CH<sub>2</sub>=CH–CH=CH<sub>2</sub>; Air Products and Chemicals, Inc.) was passed through successive beds of Ascarite<sup>®</sup> II (sodium hydroxide-coated silica, Aldrich) and Drierite (Fisher). The butadiene monomer was then condensed in a cold trap (–30 °C) immersed in a mixture of 2-propanol (Aldrich) and liquid nitrogen just before use. All operations involving butadiene were carried out in a fume hood. Sodium lauryl sulfate (SLS) (CH<sub>3</sub>(CH<sub>2</sub>)<sub>11</sub>SO<sub>4</sub>Na, MW = 288.4 g/mol; Texapon K-1296, Henkel), potassium persulfate (KPS) initiator (K<sub>2</sub>S<sub>2</sub>O<sub>8</sub>, MW = 270.33 g/mol; 99+%, A.C.S. reagent, Aldrich), and 4-methylhydroquinone (MHQ) (CH<sub>3</sub>OC<sub>6</sub>H<sub>4</sub>OH, MW = 124 g/mol; 99%, purified grade, Aldrich) were used as received. Distilled–deionized (DDI) water was boiled for 15 min and then cooled to room temperature while purging with nitrogen (Zero Grade, JWS Technologies) before use to remove dissolved oxygen that might inhibit the reaction.

**Polymerization Procedures.** All latexes were prepared by batch emulsion polymerization based on the model recipe shown in Table 1. High-pressure glass reaction bottles were used to prepare the latexes because butadiene monomer is a gas at STP. A series of 42 mL bottles were employed with 73% of the volume initially filled with the reaction mixture according to the recipe. Each bottle was used to obtain data at a different reaction time for a given recipe and reaction conditions. Before use, the bottles were purged with nitrogen to displace the air. The styrene and acrylic acid monomer and the SLS and initiator solution in DDI water were transferred to each bottle and kept in ice–water before the addition of the butadiene monomer. The latter was condensed in a siphoning Schlenk tube cooled by a mixture of liquid nitrogen and 2-propanol and then transferred to each bottle (by weight with an excess of about ~0.5 g). The bottles were capped with a rubber gasket and a metal crown cap. A syringe needle was inserted through a hole in the cap to release the excess butadiene until the desired amount was attained. The bottles were then placed in a temperature-controlled water bath and rotated end-over-end at 22 rpm. During the polymerization, bottles were removed at various reaction times (representing different conversions) and cooled in an ice bath to quickly slow the reaction. The polymerization was completely stopped by injecting 0.5 mL of a 2% 4-methylhydroquinone aqueous solution into each bottle.

**Latex Characterization. a. Conversion.** Because of the volatility of the butadiene, a special method is required for the measurement of conversion. This method is described as follows. After polymerization and injection of the MHQ solution, the bottles having different conversions were weighed and then depressurized by inserting a syringe needle in order to release the unreacted butadiene monomer. The bottles were weighed again to obtain the amount of lost monomer by depressurization ( $W_{\text{los}}$ ). A latex sample of 1.0–1.5 mL was taken from each reaction bottle using a syringe and injected into a 2 oz vial, which was then immediately sealed and weighed again to obtain  $W_{\text{wet}}$ . The latex samples contained in the vials were dried in a vacuum oven at 60 °C to a constant weight. The conversion of each sample was calculated accord-

ing to the following equation:

$$\% \text{ conversion} = \frac{\{W_{\text{dry}}/[W_{\text{wet}} + (W_{\text{los}}/W_{\text{ef}})W_{\text{wet}}]\} - W_{\text{nor}}/W_{\text{tot}}}{W_{\text{mon}}/W_{\text{tot}}} \quad (1)$$

where  $W_{\text{dry}}$  is the weight of the latex solids in the vial after drying,  $W_{\text{wet}}$  is the weight of the latex in the vial before drying,  $W_{\text{los}}$  is the weight loss from the reaction bottle by depressurization,  $W_{\text{ef}}$  is the weight of the latex left in the reaction bottle after depressurization,  $W_{\text{nor}}$  is the weight of the nonreacting species (initiator + SLS + inhibitor),  $W_{\text{mon}}$  is the weight of the monomers (St + Bu + AA), and  $W_{\text{tot}}$  is the total weight of the materials added to the polymerization bottle. Conversions measured using this method were compared with an alternative method in which the conversion was measured by drying the entire sample contained in the bottle. The difference in percent conversion determined by the two methods was less than 1%, showing that the method we used was sufficiently accurate.

**b. Particle Size.** The average particle diameter at low conversions was too small (~10–25 nm) to be determined by dynamic light scattering (DLS) and capillary hydrodynamic fractionation (CHDF). Transmission electron microscopy (TEM, Phillips 400) was used for these particle size measurements. Prior to TEM examination, the unreacted monomers were removed from the latexes using a rotary evaporator. It was also noted that OsO<sub>4</sub> staining could not be used for samples obtained in the very early stages of polymerization (<5% conversion) due to some hindered access of the OsO<sub>4</sub> to the very small particles (<20 nm) created by a high carboxylic group concentration at the particle surface. Therefore, the particles were negatively stained by uranyl acetate to enhance their contrast, especially at low conversions. A cold stage sample holder, cooled by liquid N<sub>2</sub>, was used to harden the particles during the measurements. Typically 1000–1500 particles were measured on the micrographs using a Zeiss Mop-3 analyzer. The volume-average diameter,  $D_v$ , was determined from these measurements, which was then used to calculate the number of particles,  $N_p$  (per liter of water):

$$N_p = \frac{6X(M/W)}{\pi\rho D_v^3} \quad (2)$$

where  $X$  is the fractional conversion, ( $M/W$ ) the monomer-to-water weight ratio, and  $\rho$  the polymer density ( $\rho = 0.98 \text{ g cm}^{-3}$ ; average density of the copolymer).

**c. Unreacted Acrylic Acid Monomer in Latex.** Gas chromatography (GC) is a commonly used method to determine the residual amount of monomers in latexes. The direct analysis of residual AA in the latex by gas chromatography had not been previously successful.<sup>2</sup> This is because acidic compounds generally form hydrogen bonds due to their high polarity, and as a result they are often strongly adsorbed in the GC column. Consequently, they result in tailing or poorly resolved peaks and contaminate the column.

In general, a possible means of analyzing latex samples for residual AA is by derivatizing the samples before analysis to obtain the acrylic acid ester. Trimethylanilinium hydroxide (TMAH), also known as trimethylphenylammonium hydroxide, has been successfully used in the derivatization and analysis of mixtures of long-chain carboxylic acids (e.g., oleic acid) by Briones et al.,<sup>3</sup> in the presence of large quantities of water where the acid was partially emulsified.

The addition of TMAH to a sample containing fatty acids forms fatty acid–TMAH salts. Direct injection of this solution into a hot (260–300 °C) GC injection port results in pyrolytic methylation of the fatty acid, yielding the fatty acid methyl esters.

The internal standard chosen for the determination of both styrene and acrylic acid was dioxane. Before GC injection, the acrylic acid monomer was preneutralized by using a 0.1 M TMAH in methanol solution.

**Aqueous Phase Characterization. a. Separation of the Aqueous Phase from Particle Phase.** It was important to find a method of separating the aqueous phase containing the oligomers from the particles without affecting the oligomer partitioning in the system. Among the commonly used separation methods are solvent extraction, high-pressure filtration, serum replacement, and ultracentrifugation. The latter is based on the difference in densities between the particle and the serum phases. Therefore, it appeared to be a good choice for separating the serum phase without disturbing the oligomer partitioning, especially for the samples obtained in the early stages of a polymerization.

To obtain consistent separation results for all the samples having different conversions, the centrifugation conditions were fixed for all the systems studied. In general, better separation results can be achieved by increasing both rpm and time. The centrifuge speed was set at the maximum as determined by the rotor, namely 37 000 rpm. The criterion for determining the centrifugation time was that the aqueous phase at the bottom of the centrifuge tubes should be clear for all conversions. It was noted that as the conversion increased it became exceedingly more difficult to achieve this. For samples with conversions greater than 80%, increasing the time from 36 to 48 h, and even up to 72 h, did not result in a clear aqueous phase. Since this study is focused on the earliest stages of the polymerization, 36 h was selected as the optimum centrifugation time and used for all the systems investigated here.

After ultracentrifugation, the clear serum was carefully removed from the bottom of the tube using a syringe needle inserted through the tube wall and was then stored in a refrigerator ( $\sim 9^\circ\text{C}$ ).

Information about the variation in the amount and composition of the water-soluble oligomers formed in the aqueous phase as a function of conversion will be determined by quantitative NMR measurements as discussed below.

**b. Preparation of Serum Samples.** Based on the recipe and the polymerization process, the serum can contain water-soluble oligomers that may consist of St, Bu, and AA monomeric units, surfactant, unreacted AA monomer, inhibitor (MHQ), and initiator.  $^1\text{H}$  NMR was used for quantitative determination of the composition of the water-soluble oligomers and their concentration in the serum. Prior to making any NMR measurements, the  $\text{H}_2\text{O}$  content in the serum has to be reduced. However, a problem encountered here was that the dried solids obtained from the serum after drying in a vacuum oven, or even after freeze-drying, could not be redissolved in  $\text{D}_2\text{O}$ . If the pH was adjusted to above 10, to fully neutralize the AA (thus limiting the formation of hydrogen bonds during drying), only part of the solids could be dissolved in  $\text{D}_2\text{O}$ . This phenomenon indicated that there may be some kind of cross-linking reaction involving the residual double bonds in the butadiene component of the polymer chains under low oxygen conditions, which resulted in polymer that could not be dissolved in water or any solvent. A special method to evaporate the  $\text{H}_2\text{O}$  without cross-linking the serum oligomers was developed to prepare the serum samples for  $^1\text{H}$  NMR measurements, as described in the following.

A known amount of serum ( $\sim 2$  g) was placed in a vial and stirred by a magnetic stirrer.  $\text{N}_2$  was blown over the top of the serum surface to evaporate off the  $\text{H}_2\text{O}$ , concentrating the serum (to  $\sim 0.5$  g). About 1 g of  $\text{D}_2\text{O}$  was added to the serum, and the mixture was concentrated again to around 0.5 g. After repeating this procedure twice, the remaining  $\text{H}_2\text{O}$  in the serum is small enough for  $^1\text{H}$  NMR measurements to be made without influencing the analysis of the serum composition (see water peaks in Figure 1). After the exchange, the serum enriched in  $\text{D}_2\text{O}$  was fully neutralized by adding a solution of NaOH in  $\text{D}_2\text{O}$  to neutralize the carboxylic groups present in the oligomer chains, which can increase the water solubility of the oligomers and disrupt hydrogen bond formation.

**c.  $^1\text{H}$  NMR Measurements.** After the preceding step was complete, the sera were transferred to 5 mm diameter NMR glass tubes. A known amount of 3-(trimethylsilyl)tetradeuteriosodium propionate (TSP) ( $(\text{CH}_3)_3\text{SiCD}_2\text{CD}_2\text{COONa}$ ) was

added to each sample as an internal standard, which gives a zero chemical shift ( $\delta = 0.00$  ppm) in  $^1\text{H}$  NMR. The  $^1\text{H}$  NMR analyses were carried out using a 500 MHz NMR instrument (Bruker). The  $^1\text{H}$  NMR spectra of all serum samples were recorded by the spectrometer operating at 500.17 MHz at  $25^\circ\text{C}$ . The recording conditions were as follows: spectral width, 6024 Hz with a  $23^\circ$  pulse angle; acquisition time, 2.72 s; pulse repetition, 10 s; number of data points (FID), 32K; and number of scans, 150–180, depending on the sample. All chemical shifts were referenced to TSP.

Figure 1 presents the  $^1\text{H}$  NMR spectrum of the serum separated from a St/Bu/AA latex sample taken at 9.6% conversion (4 mol % AA,  $70^\circ\text{C}$ , and 32 mM SLS) by using 0.3 Hz line broadening. The  $^1\text{H}$  NMR peak assignments of the species in the serum are based on the  $^1\text{H}$  NMR spectrum of standard samples such as MHQ, AA, PAA, PBu, PSt, and SLS. Peak  $A_1$  is assigned to the aromatic protons in the benzene ring of the PSt and MHQ (in both reacted and unreacted MHQ). Peak  $A_2$  is assigned to the  $\text{H}_\alpha$  protons and one  $\text{H}_\beta$  double-bond proton of the acrylic acid monomer. Peak  $A_3$  represents the double-bond protons and that of another  $\text{H}_\beta$  of the AA monomer (the sharp peak at  $\sim 5.45$  ppm). The strong peak at  $\sim 4.3$  ppm is the HOD and HOH protons from water. Two protons from the methylene ( $\text{CH}_2$ ) group directly linked to the sulfate group in SLS are represented as peak  $A_4$ . The other methylene protons in SLS are shown in peak  $A_7$  as well as all the protons from  $\text{CH}_2$  and  $\text{CH}$  in the PAA, PBu, and PSt. Peaks  $A_5$  and  $A_6$  are the  $\text{CH}_3$  protons in MHQ, reacted and unreacted, respectively. The nine methyl protons in the internal standard (TSP) are assigned as peak  $A_8$ .

On the basis of the relationship between the peak area and the number of moles of protons involved in each peak, the serum composition was analyzed quantitatively by solving the following equations, where  $A_i$  represents the peak areas shown in Figure 1 and  $M_i$  is the number of moles of each proton.

$$A_1 = 5M_{\text{PSt}} + 3M_{\text{MHQ}}^{\text{Re}} + 4M_{\text{MHQ}}^{\text{UR}} \quad (3)$$

$$A_2 = 2M_{\text{AA}} \quad (4)$$

$$A_3 = 2M_{\text{CT}} + 3M_{\text{V}} + M_{\text{AA}} \quad (5)$$

$$A_4 = 2M_{\text{SLS}} \quad (6)$$

$$A_5 = 3M_{\text{MHQ}}^{\text{UR}} \quad (7)$$

$$A_6 = 3M_{\text{MHQ}}^{\text{Re}} \quad (8)$$

$$A_7 = 3M_{\text{PSt}} + 3M_{\text{PAA}} + 3M_{\text{V}} + 20M_{\text{SLS}} \quad (9)$$

$$A_8 = 9M_{\text{TSP}} \quad (10)$$

where  $M_{\text{MHQ}}^{\text{UR}}$  represents the moles of unreacted MHQ and  $M_{\text{MHQ}}^{\text{Re}}$  represents the moles of reacted MHQ.  $M_{\text{CT}}$  represents the moles of both *trans*- and *cis*-polybutadiene. Since  $M_{\text{PBu}} = M_{\text{CT}} + M_{\text{V}}$  and  $M_{\text{V}} = 0.15M_{\text{Bu}}$ ,<sup>4</sup> the number of moles can be obtained:

$$M_{\text{PSt}} = 1/5(A_1 - A_6 - 4/3A_5) \quad (11)$$

$$M_{\text{PBu}} = 1/1.215(A_3 - A_2/2) \quad (12)$$

$$M_{\text{SLS}} = 1/2A_4 \quad (13)$$

$$M_{\text{PAA}} = 1/3(A_7 - 3.85M_{\text{PBu}} - 3M_{\text{PSt}} - 20M_{\text{SLS}}) \quad (14)$$

$$M_{\text{TSP}} = 1/9A_8 \quad (15)$$

Then, the mole concentration and weight percent of each species in the aqueous phase can be calculated by using the known molar concentration of the internal standard (TSP).



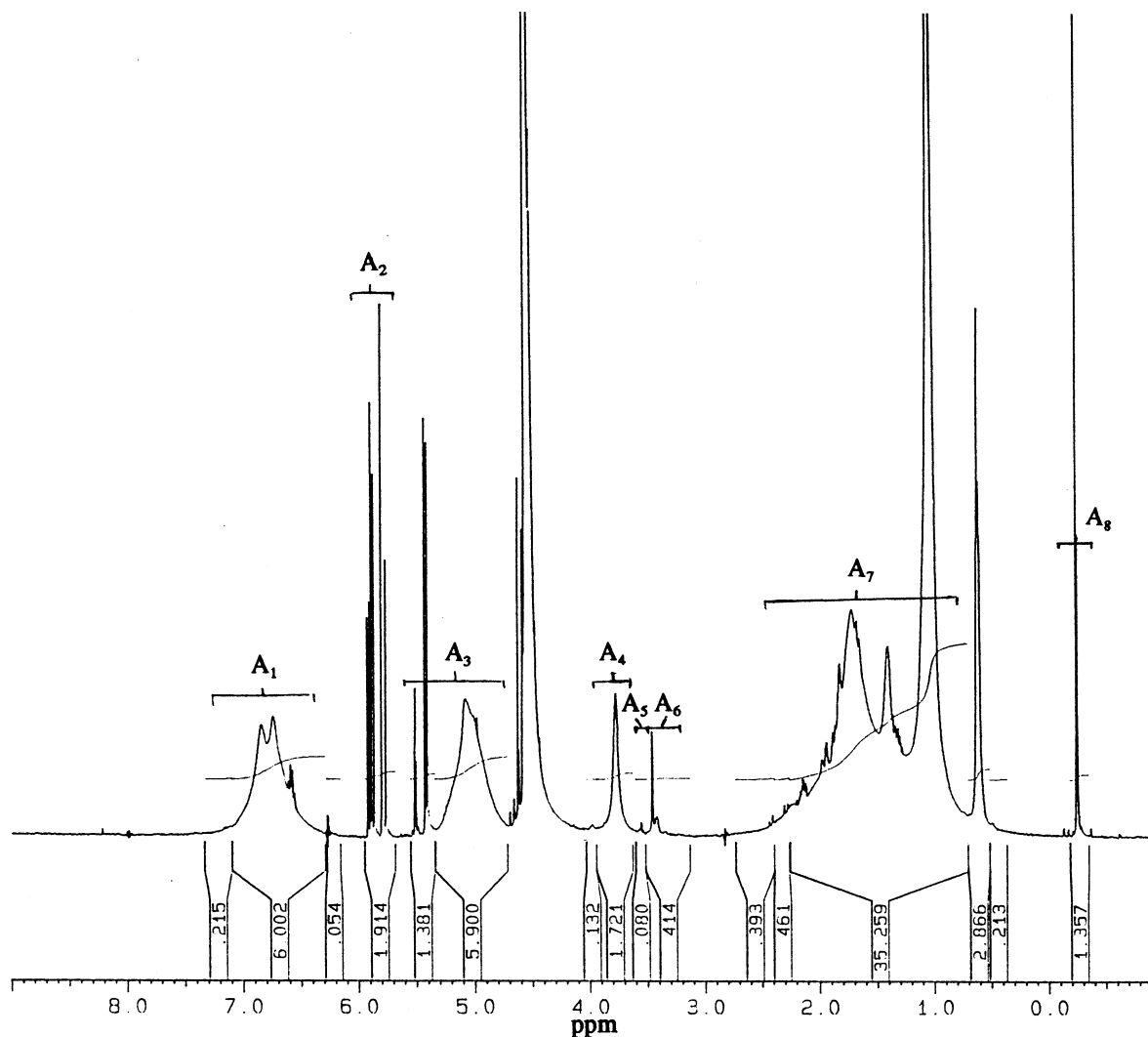


**Figure 1.**  $^1\text{H}$  NMR spectrum of serum (taken at 9.6% conversion, 4 mol % AA, and 32 mM SLS from the model St/Bu/AA emulsion polymerization system): peak A<sub>1</sub>, aromatic proton of PSt and MHQ; peak A<sub>2</sub>, H <sub>$\alpha$</sub>  and H <sub>$\beta$</sub>  protons of AA; peak A<sub>3</sub>, PBU  $-\text{CH}=\text{CH}-\text{CH}=\text{CH}_2$  protons and one H <sub>$\beta$</sub>  proton of AA; peak A<sub>4</sub>, SLS  $-\text{CH}_2-\text{SO}_4^-$  protons; peak A<sub>5</sub>,  $\text{CH}_3-$  protons of unreacted MHQ; peak A<sub>6</sub>,  $\text{CH}_3-$  protons of reacted MHQ; peak A<sub>7</sub>,  $\text{CH}_2$ ,  $\text{CH}$  protons from PAA, PBU, PSt, and SLS; peak A<sub>8</sub>,  $\text{CH}_3-$  protons of TSP (internal standard).

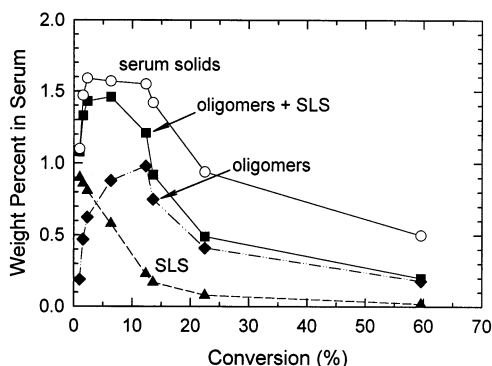


**Figure 2.** Weight percent of water-soluble oligomers, surfactant (SLS), oligomers plus surfactant, and serum solids content as a function of conversion for a St/Bu/AA emulsion polymerization carried out with [AA] = 4 mol %, [I] = 3.17 mM + 3.17 mM KCl, and [SLS] = 32 mM;  $T_r$  = 70 °C.

The results obtained for the amount of oligomers and surfactant in the serum as well as their sum determined by  $^1\text{H}$  NMR as a function of conversion were compared with the serum solids content results obtained gravimetrically. The results, for example as shown in Figure 2, indicate a reasonable match, although the solids content measurement always exceeds that obtained through NMR.

**Oligomer Molecular Weight Measurement.** The molecular weights of the water-soluble oligomers in the serum were determined by aqueous phase gel permeation chromatography (GPC). Two size exclusion HPLC columns (Varian Micropak TSKgel), PX<sub>XL</sub>2500 and PW4000, were used, and 0.01 M  $\text{NaNO}_3$  aqueous solution was used as the mobile phase. A GPC instrument (Waters) with a refractive index detector, operated at a flow rate of 0.8 mL/min, was used to carry out the separations. The columns were calibrated using water-soluble polymer standards of poly(ethylene oxide) with molecular weights in the range of 660–37 000 (Polymer Laboratories, Inc.). The calibration curve is shown in Figure 3. The Mark–Houwink constants of PAA, shown in Table 2, were used to determine the molecular weight of the oligomers in reference to PEO. Before injecting into the GPC, each serum sample was filtered through a 0.45  $\mu\text{m}$  cellulose acetate (CA) filter and fully neutralized by adding aqueous NaOH solution (to decrease the adsorption of oligomers and AA on the column packing material). A GPC chromatogram of neutralized water-soluble oligomers and acrylic acid in the serum is shown in Figure 4. The oligomer peak overlaps the peak of the neutralized AA owing to the limitations in the column separation. The molecular weight at the beginning of the first peak is taken as the maximum molecular weight ( $\text{MW}_{\text{max}}$ ), and the one at the first peak position can be taken as the oligomer molecular weight of the greatest amount of material ( $\text{MW}_{\text{peak}}$ ) in each serum sample.

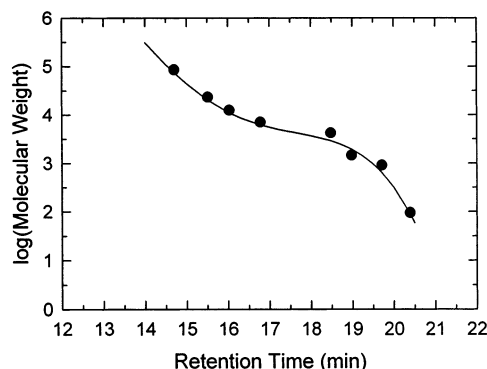


**Figure 3.** GPC calibration curve using PEO standards.

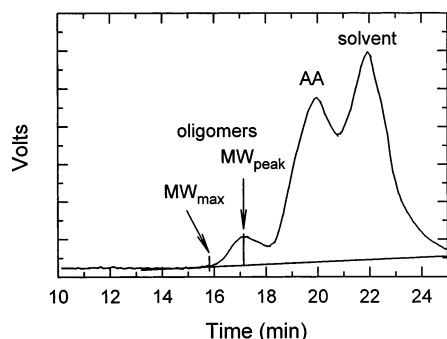


**Figure 4.** GPC chromatogram of neutralized water-soluble oligomers and acrylic acid (AA) in the serum.

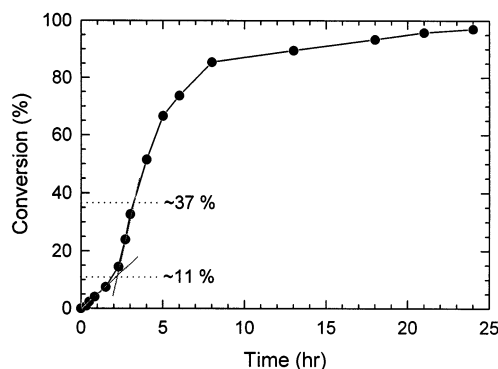


**Figure 5.** Conversion vs time for the St/Bu/AA (39/57/4 mol %) model emulsion polymerization system carried out with [SLS] = 32 mM, [AA] = 4 mol %, and [I] = 3.17 mM;  $T_r = 70^\circ\text{C}$ .

**Table 2.** Mark–Houwink Constants<sup>4</sup> Used in the Gel Permeation Chromatography Molecular Weight Determinations

polymer	medium	$k$	$a$
poly(ethylene oxide)	water	0.0125	0.78
poly(acrylic acid)	0.01 N NaBr aqueous solution	0.0132	0.91

## Results and Discussion

**Model System. a. Kinetic Behavior.** In accordance with the model recipe (4 mol % acrylic acid) given in Table 1, an emulsion polymerization was carried out by batch polymerization at  $70^\circ\text{C}$ . The conversion vs time results are presented in Figure 5. The polymerization eventually goes to  $\sim 98\%$  conversion after 32 h reaction (not shown in Figure 5). The number of particles and their weight-average diameter ( $D_w$ ) vs conversion curves are shown in Figure 6.

The conversion–time curve has a characteristic S-shape. Since the slope of the curve indicates the rate of

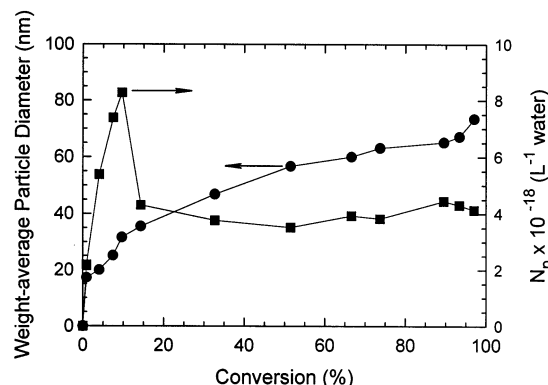


**Figure 6.** Weight-average particle diameter ( $D_w$ ) and number of particles per liter water ( $N_p$ ) vs conversion for the St/Bu/AA (39/57/4 mol %) model emulsion polymerization system carried out with [SLS] = 32 mM, [AA] = 4 mol %, and [I] = 3.17 mM;  $T_r = 70^\circ\text{C}$ .

polymerization, three intervals can be distinguished on the basis of the changes in the slopes as shown in Figure 5. The results show that, in this model system, interval I begins with a fast increase in the number of particles and seems to end at around 11% conversion, as indicated by the first obvious change in the slope of the conversion–time curve. At this point a sharp increase in  $N_p$  is seen. Interval II, characterized by an apparent constant rate period, ends at around 37% conversion, signifying the disappearance of the monomer droplets<sup>5</sup> and the resulting decrease in the rate of polymerization ( $R_p$ ). Interval III, according to Harkins,<sup>6</sup> should start from the point at which  $R_p$  begins to decrease until the end of the polymerization.

In this model system,  $N_p$  increased rapidly with increasing conversion during interval I. After reaching a maximum value of  $\sim 8.4 \times 10^{18}$  (particles per liter of water) at  $\sim 10\%$  conversion (which should represent the end of particle nucleation and the end of interval I, as will be discussed later), it dropped sharply until it reached a new value of  $\sim 4.3 \times 10^{18}$  ( $\text{L}^{-1}$  water) at  $\sim 14\%$  conversion and then remained nearly constant during intervals II and III. The increase in  $N_p$  represents the fast generation of particles during the particle nucleation period. On the other hand, the decrease in  $N_p$  indicates a limited aggregation of the growing particles, which results in a corresponding increase in particle size. According to Yeliseyeva,<sup>7</sup> the limited aggregation of primary particles depends on the ratio of the rate of formation of their overall surface ( $s$ ) to the rate of establishment of equilibrium adsorption ( $\Gamma$ ) of the emulsifier on the surface. For the formation of particles stabilized by an emulsifier,

$$d\Gamma/dt = K ds/dt \quad (16)$$

where  $K$  is a proportionality constant which takes into account the value of equilibrium adsorption. In reality, however, it may be that

$$d\Gamma/dt < K ds/dt \quad (17)$$

where the surface area is created faster than equilibrium adsorption can be achieved.

Depending on whether the condition of eq 16 is met, the course of particle formation will vary. When this condition is satisfied, the surface formed by the polymer phase is stabilized by the adsorbing emulsifier. In the

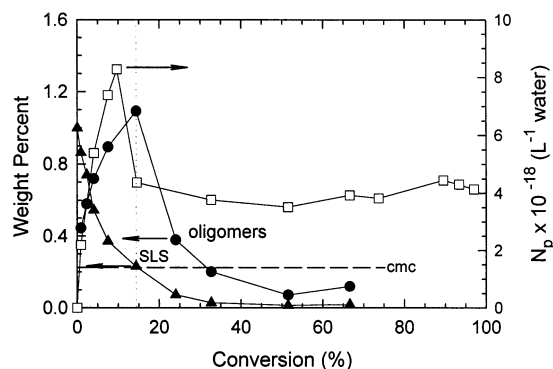


**Figure 7.** Number of particles ( $N_p$ ) and the concentration (weight percent) of water-soluble oligomers and surfactant in the aqueous phase vs conversion for the St/Bu/AA (39/57/4 mol %) model emulsion polymerization carried out with [SLS] = 32 mM, [AA] = 4 mol %, and [I] = 3.17 mM;  $T_r = 70^\circ\text{C}$ .

case of the inequality, as expressed in eq 17, for example at high polymerization rates, particles appear whose surface is insufficiently protected by the emulsifier, and flocculation occurs. Such particles will rapidly flocculate with each other, and a new equilibrium adsorption of the emulsifier is established on the aggregated and coalesced latex particles. Therefore, under these circumstances, the study of the variation of surfactant concentration and the amount and composition of the water-soluble oligomers during this period would be helpful in understanding particle formation. This will be shown in the following discussion.

**b. Aqueous Phase Characterization.** With the addition of a highly water-soluble monomer such as acrylic acid to a low water-solubility monomer system (St/Bu), significant reaction of this monomer is expected in both aqueous and particle phases due to the partitioning of the water-soluble monomer between the two phases. The  $^1\text{H}$  NMR analysis revealed that the water-soluble oligomers found in the aqueous phase for the St/Bu/AA model system consist of all three monomer units, namely styrene, butadiene, and acrylic acid, as shown in Figure 1. The concentrations (weight percent) of water-soluble oligomers, as well as surfactant, in the aqueous phase as a function of conversion are presented in Figure 7. The results reveal that the concentration of water-soluble oligomers increased and the concentration of SLS decreased with increasing conversion at the beginning of the polymerization ( $X < 15\%$ ). As the surfactant concentration decreased to levels below the critical micelle concentration (cmc), the oligomer concentration reached a maximum and then rapidly decreased to a low value.

It should be mentioned that the true cmc of the surfactant in the actual emulsion polymerization system is difficult to determine, owing to the complexity of the effect of many parameters on the cmc value, as discussed by Rosen.<sup>8</sup> According to the law of mass action, the cmc is not a single value of the surfactant concentration but a narrow region. Therefore, an approximate value can be obtained either by experimental determination (i.e., soap titration<sup>9</sup>) or by calculation.<sup>10,11</sup> The cmc of SLS in this system with 6.34 mM  $\text{K}^+$  ions (from 3.17 mM  $\text{K}_2\text{S}_2\text{O}_8$  initiator) is 7.1 mM ( $= 0.22 \text{ g}/100 \text{ g}$  of serum), as represented by the dashed line in Figure 7, which was calculated using eq 18:<sup>12</sup>

$$\log \text{cmc} = A - K_0 \log C_i \quad (18)$$

where  $A$  and  $K_0$  are constants ( $-3.6$  and  $0.66$  for SLS, respectively).  $C_i$  is the concentration of counterions.

To better relate the behavior in the aqueous and particle phases during the reaction, the  $N_p$  vs conversion curve is also plotted in Figure 7. The results show that, during the particle generation period, the rapid increase in  $N_p$  was accompanied by a fast decrease in the aqueous SLS concentration. As the number of micelles decreased,  $N_p$  reached its maximum value. In this case, it would seem that the rate of establishment of equilibrium adsorption of the surfactant on the particles was slower than the rate of formation of the overall particle surface, and therefore, limited flocculation occurred as the aqueous SLS concentration approached its cmc. There have been many studies documenting the interactions existing between water-soluble polymers and surfactants in aqueous solutions.<sup>13,14</sup> When mixed together in aqueous solution, a complex formation takes place by binding of the surfactants onto the polymer chains. Therefore, in the presence of water-soluble oligomers, SLS molecules can form a surfactant-polymer complex, and consequently the concentration of free SLS in the continuous phase will decrease. Under such conditions, micelle depletion will take place at an overall SLS concentration even slightly higher than that of the cmc in the absence of water-soluble polymer.

The results obtained in Figure 7 also show that, after  $N_p$  began to decrease, the concentration of water-soluble oligomers in the aqueous phase also decreased. The reason for this decrease may be explained as follows. Under the polymerization conditions of the model system (i.e., [SLS] > cmc and [AA] = 4 mol % on monomer), both micellar-entry and homogeneous-coagulative nucleation should both be considered to explain the particle formation mechanism.<sup>15</sup> Precursor particles are formed either by micellar or by homogeneous nucleation at the beginning of the reaction. As depicted in the schematic representation of the micellar and the homogeneous-coagulative nucleation theories given in Figure 8, in this case, several competitive processes should be involved that affect the formation of particles as well as oligomers in the aqueous phase, whose rates are  $R_{p,aq}$  (the rate of radical propagation in the aqueous phase),  $R_{mic}$  (the rate of radical entry into micelles resulting in the formation of primary particles),  $R_{pri}$  (the rate of the radical precipitation to form primary particles by homogeneous nucleation),  $R_{cap}$  (the rate of oligomeric radical capture by existing particles),  $R_{t,w-s}$  (the rate of oligomeric radical termination to form water-soluble dead oligomers),  $R_{t,w-ins}$  (the rate of radical termination to form water-insoluble oligomers which then precipitate out to form particles,  $R_{t,pri}$ , or adsorb onto existing particles,  $R_{ads}$ ),  $R_{coag}$  (the rate of the particle coagulation),  $R_{des}$  (the rate of desorption of the oligomeric radicals from both micelles and particles), and  $R_{ads}$  (the rate of oligomer adsorption onto the particles). The variation in  $N_p$  and the concentration of water-soluble oligomers in the aqueous phase can be explained by examining these terms.

The number of particles ( $N_p$ ) in the latex will increase directly with an increase in  $R_{mic}$ ,  $R_{pri}$ , and  $R_{t,pri}$ , and it will decrease with increasing  $R_{coag}$ . Changes in  $R_{p,aq}$ ,  $R_{cap}$ ,  $R_{t,w-s}$ ,  $R_{des}$ , and  $R_{ads}$  will not change  $N_p$  directly. Therefore, the net rate of particle formation can be presented as

$$dN/dt = (R_{mic} + R_{pri} + R_{t,pri}) - R_{coag} \quad (19)$$

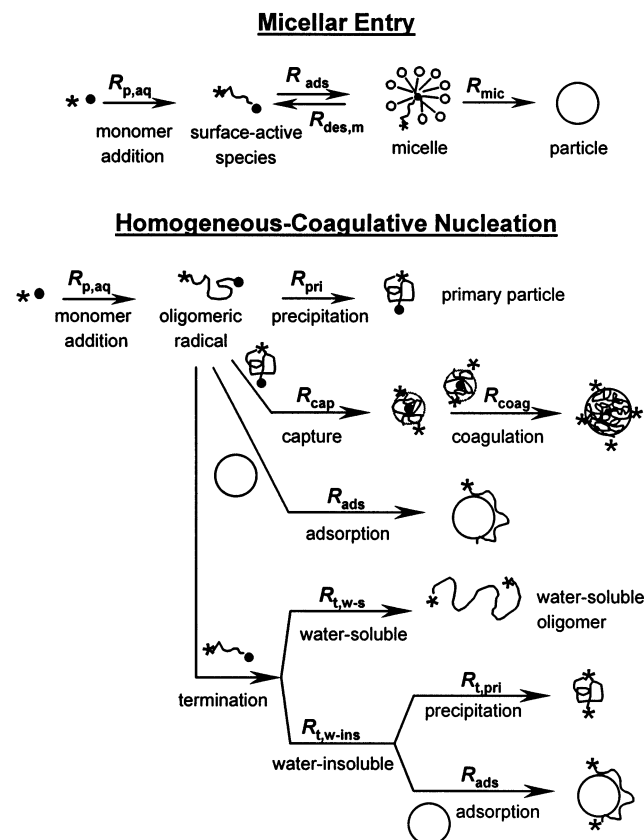


**Figure 8.** Schematic representation of the micellar and homogeneous-coagulative nucleation theories.

The formation of particles and oligomers in this model system can now be explained on the basis of the experimental results shown in Figure 7. At the very beginning of the reaction

$$R_{mic} + R_{pri} + R_{t, pri} > R_{coag} \quad (20)$$

This resulted in the rapid increase in the number of particles with increasing conversion. Meanwhile, the growing surface area of the newly formed particles led to the rapid decrease in the surfactant concentration in the aqueous phase (see Figure 7).

As particles continued to be formed, the free surfactant concentration in the aqueous phase decreased to near the cmc. The stability of the newly formed particles will be highly dependent on the rate of establishment of equilibrium adsorption of the emulsifier on the particle surface ( $d\Gamma/dt$ ), which would be decreased when the micelle concentration is limited. Therefore,  $R_{coag}$  and  $R_{t, pri}$  would increase and  $R_{mic}$  would decrease (finally decreasing to zero as the emulsifier concentration in the aqueous phase decreases to below the cmc). The difference between  $(R_{mic} + R_{pri} + R_{t, pri})$  and  $R_{coag}$  will decrease to zero at the maximum  $N_p$  (i.e.,  $dN/dt = 0$  at  $\sim 11\%$  conversion). After that, the coagulation rate will increase due to insufficient surfactant to stabilize the growing particles. Therefore,  $R_{pri} + R_{t, pri} < R_{coag}$ , and  $N_p$  decreases. Limited coagulation occurs until a new "stabilization" condition is reached. During interval II, a nearly constant  $N_p$  was found, implying that  $R_{pri} + R_{t, pri} \approx R_{coag}$ .

On the other hand, the concentration of the free water-soluble oligomer species in the aqueous phase will increase directly with increases in  $R_{p, aq}$ ,  $R_{des}$ , and  $R_{t, w-s}$ . It will decrease with increases in  $R_{pri}$ ,  $R_{mic}$ ,  $R_{cap}$ ,  $R_{ads}$ ,

and  $R_{t, pri}$ , and is not affected by varying  $R_{coag}$ . Therefore, the net rate of formation of the free water-soluble oligomers in the aqueous phase can be presented as

$$dC_{oli}/dt = (R_{p, aq} + R_{des} + R_{t, w-s}) - (R_{pri} + R_{mic} + R_{cap} + R_{t, pri} + R_{ads}) \quad (21)$$

where  $C_{oli}$  represents the concentration of the water-soluble oligomers in the aqueous phase. At the very beginning of the polymerization, a relatively large amount of free radicals are formed by decomposition of the initiator, which subsequently add monomer units forming oligomeric radicals. In this case,  $R_{p, aq}$  and  $R_{des}$  are high, while the terms in the right parentheses are relatively small. Therefore,

$$R_{p, aq} + R_{des} + R_{t, w-s} > R_{pri} + R_{mic} + R_{cap} + R_{t, pri} + R_{ads} \quad (22)$$

The total amount of water-soluble oligomers increases with conversion to a maximum ( $\sim 14\%$  conversion according to the experimental data obtained in Figure 7). As more particles are formed in the system,  $R_{cap}$ ,  $R_{ads}$ ,  $R_{t, w-s}$ , and  $R_{t, pri}$  would increase. Therefore, the amount of free water-soluble oligomers in the aqueous phase reaches a maximum value, where  $dC_{oli}/dt = 0$ , and

$$R_{p, aq} + R_{des} + R_{t, w-s} = R_{pri} + R_{mic} + R_{cap} + R_{t, pri} + R_{ads} \quad (23)$$

After the emulsifier concentration in the aqueous phase is reduced to below the cmc ( $R_{mic} = 0$ ),  $R_{cap}$  and  $R_{ads}$  will be further increased as more mature particles are formed and continue to grow in the system. On the other hand, the rate of desorption of oligomeric radicals from the particle surface must decrease as more mature particles are formed because of the relatively stronger hydrophobic interaction of oligomers with the long-chain polymers in the particle phase. All of this would result in

$$R_{p, aq} + R_{des} + R_{t, w-s} < R_{pri} + R_{cap} + R_{t, pri} + R_{ads} \quad (24)$$

and a decrease in the amount of the water-soluble oligomers in the aqueous phase after the decrease in  $N_p$ .

It should be pointed out that the water-soluble oligomers found in the aqueous phase should contain both water-soluble oligomeric radicals terminated by the inhibitor (MHQ) and dead water-soluble oligomers formed by aqueous phase termination of two oligomeric radicals. When the surfactant concentration is above the cmc, oligomeric radicals will enter and exit both micelles and particles. The desorption of oligomeric radicals and dead oligomers from the surface of polymer particles is expected to be more difficult compared to micelles (when they exist).

If we consider the evolution of the oligomer composition and molecular weight with increasing conversion, the reason for the decrease in oligomer concentration can be further understood. Figure 9 shows the variation with conversion of the mole percent of St, Bu, and AA monomer units present in the water-soluble oligomers, and Figure 10 shows the GPC chromatograms obtained for the water-soluble oligomers as a function of conversion. These results show that the composition and



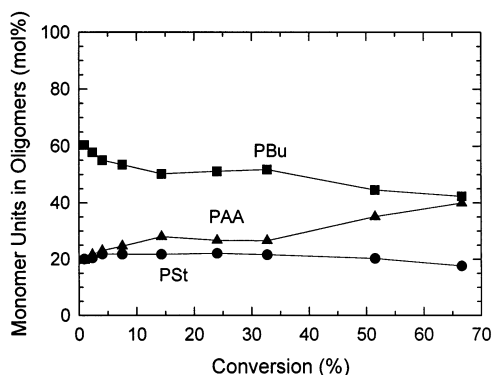


**Figure 9.** Mole percent of St, Bu, and AA monomeric units present in the water-soluble oligomers vs conversion for the model St/Bu/AA (39/57/4 mol %) emulsion polymerization carried out with [SLS] = 32 mM, [AA] = 4 mol %, and [I] = 3.17 mM;  $T_r = 70^\circ\text{C}$ .

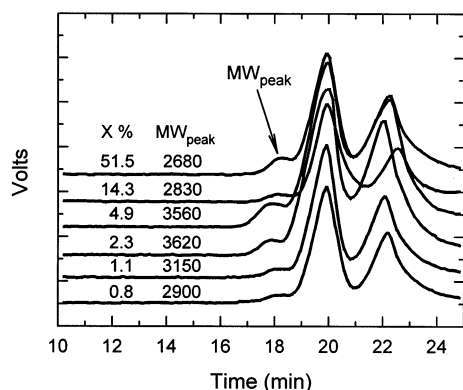


**Figure 10.** GPC chromatograms of the water-soluble oligomers and peak molecular weights as a function of conversion for the model St/Bu/AA (39/57/4 mol %) emulsion polymerization carried out with [SLS] = 32 mM, [AA] = 4 mol %, and [I] = 3.17 mM;  $T_r = 70^\circ\text{C}$ .

molecular weight of the water-soluble oligomers varied during the polymerization. It is reasonable to believe that both the adsorption and desorption of oligomers from the particle surface depend on the composition and molecular weight of the oligomers. At the end of interval I, those oligomers rich in St and Bu monomeric units and with relatively long chain lengths would prefer to stay in the particle phase because they have a stronger interaction (hydrophobic) with the particles compared to those oligomers rich in AA units and have shorter chain lengths as found in the aqueous phase.

As shown in Figure 9, the composition of the water-soluble oligomers was higher in PBu than in PAA, especially in the early stages of the polymerization. This was completely unexpected. Any explanation for this result must come from the mechanism of water-soluble oligomer formation and will be further investigated.

**Effect of Acrylic Acid Concentration.** As discussed above, the amount of water-soluble oligomers in the aqueous phase, as well as the number of particles ( $N_p$ ), was found to quickly increase during the particle nucleation period. The dependence of the rate of water-soluble oligomer formation on the AA concentration during this period was investigated further in the following study.

Two additional reactions with 0 and 8 mol % AA were run based on the model recipe modified by changing the AA concentration but keeping the same total monomer concentration (30% solids content) and the same mole

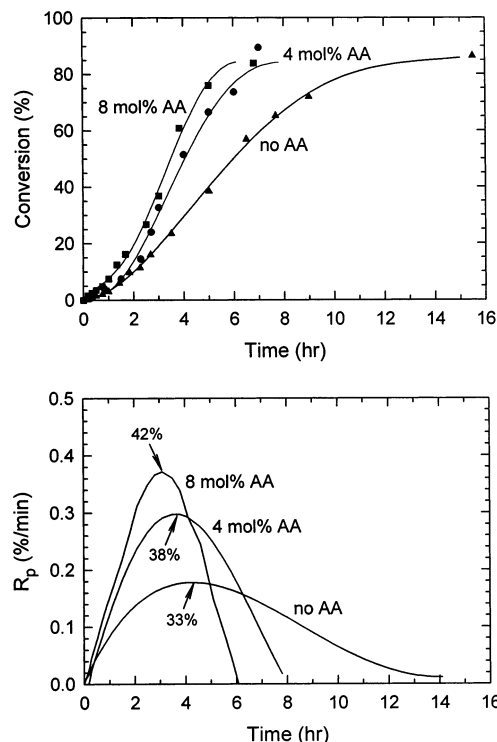


**Figure 11.** Conversion (measured gravimetrically) (top) and rate of polymerization (derivative of curve fit) (bottom) vs time for [AA] = 4 mol % (St/Bu/AA = 39/57/4 mol %), 8 mol % (St/Bu/AA = 37.5/54.5/8 mol %), and St/Bu + acetic acid (AcA) with [AA] = 0 mol % (St/Bu/AA = 49/51/0 mol %) emulsion polymerizations carried out with [SLS] = 32 mM and [I] = 3.17 mM;  $T_r = 70^\circ\text{C}$ .

**Table 3. Synthesis Conditions**

sys-tem	$T$ ( $^\circ\text{C}$ )	[I] (mM)	[SLS] (mM)	[AA] (mol %)	notes
1	70	3.17	32	0	St/Bu (41/59 mol %) + AcA
2	70	3.17	32	4	St/Bu/AA (39/57/4 mol %)
4	70	3.17	32	8	St/Bu/AA (37.5/54.5/8 mol %)

ratio of styrene and butadiene monomers (St/Bu = 39/57 mole ratio). For the system without any added AA, because of the strong effect of the pH on the decomposition rate of persulfate initiator, acetic acid, which has a similar  $K_a$  and does not react with free radicals (has no double bond), was added initially in order to adjust the pH to the same value as present in the model system (4 mol % AA). These three systems are listed in Table 3.

The conversion and rate of polymerization ( $R_p$ ) vs time curves are presented in Figure 11. Obviously, the presence of the acrylic acid monomer induced the formation of an increased number of polymer particles, thereby increasing the polymerization rate. With each increase in the acrylic acid concentration, the rate of polymerization increased and the maximum  $R_p$  was reached at higher conversions. An increase in  $R_p$  was also observed in the bulk terpolymerization of St/Bu/AA compared with the bulk copolymerization of St/Bu.<sup>16</sup> Therefore, the increase in  $R_p$  as AA is added may be caused to some degree by the acrylic acid monomer partitioning into the particle phase, in addition to the increase in the number of particles. Since the concentration of AA monomer was increased in both the aqueous phase and organic (micelle and droplets) phases with increasing total acrylic acid, the rate of generation



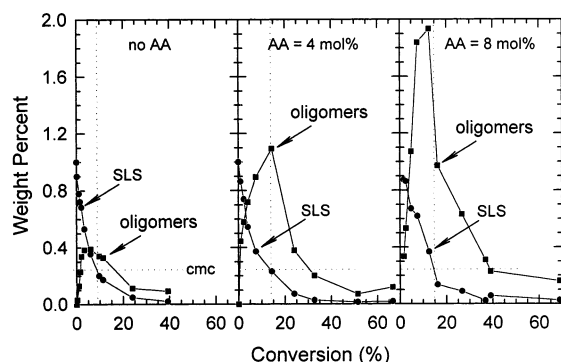


**Figure 12.** Weight percent of water-soluble oligomers and SLS in the aqueous phase vs conversion for [AA] = 4 mol % (St/Bu/AA = 39/57/4 mol %), 8 mol % (St/Bu/AA = 37.5/54.5/8 mol %), and St/Bu + acetic acid (AcA) with [AA] = 0 mol % (St/Bu/AA = 49/51/0 mol %) emulsion polymerizations carried out with [SLS] = 32 mM and [I] = 3.17 mM;  $T_r = 70^\circ\text{C}$ .

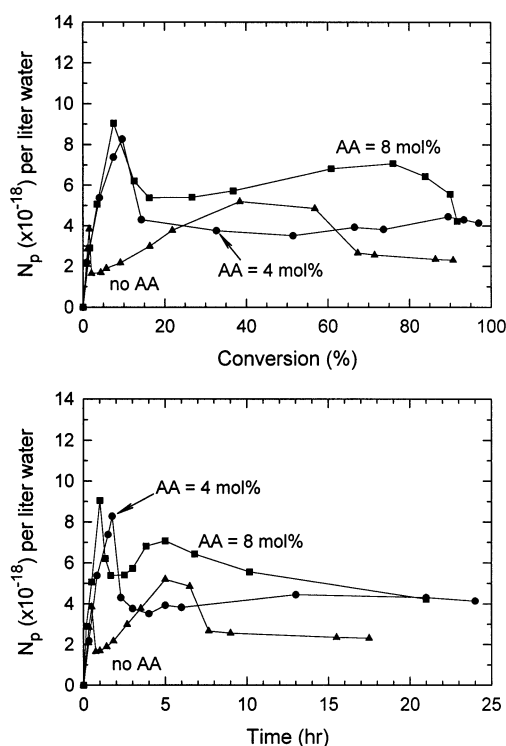


**Figure 13.** Number of particles ( $N_p$ ) vs conversion (top) and time (bottom) for [AA] = 4 mol % (St/Bu/AA = 39/57/4 mol %), 8 mol % (St/Bu/AA = 37.5/54.5/8 mol %), and St/Bu + acetic acid (AcA) with [AA] = 0 mol % (St/Bu/AA = 49/51/0 mol %) emulsion polymerizations carried out with [SLS] = 32 mM and [I] = 3.17 mM;  $T_r = 70^\circ\text{C}$ .

of oligomeric radicals and particles would be expected to increase.

The evolution of the amount of water-soluble oligomers is illustrated in Figure 12 as a function of the amount of added AA. The corresponding evolution of the number of particles ( $N_p$ ) is illustrated in Figure 13 as a function of both time and conversion. These results show that as the concentration of AA was increased in the system, the water-soluble oligomer concentration in the aqueous phase increased significantly, which indicates that more AA monomer was incorporated into the oligomers. This resulted in a faster increase in the number of particles, which can be seen clearly from the slope of the  $N_p$  vs time curves as shown in Figure 13 (bottom) for the 4 and 8 mol % AA systems.

For the case of the St/Bu/AA system, the primary particles are stabilized by emulsifier, sulfate end groups, and carboxylic acid groups. These groups are either chemically bound or adsorbed on the surface of the particles, which allows better stabilization than in the system without AA. Therefore,  $N_p$  can increase to a much higher value and limited flocculation occurs at higher conversions (10–12%) with the addition of AA. In this case, because of the existence of the hydrophilic carboxyl groups at the particle surface, less surfactant is required to stabilize each particle; therefore, more particles will be stabilized by the given surfactant.

On the other hand, for the St/Bu copolymerization carried out without AA, the primary particles are only stabilized by the surface-bound sulfate end groups from the initiator and the dynamically adsorbed emulsifier molecules. In this case, a relatively large amount of emulsifier molecules will be needed to stabilize the rapidly forming small particles. Furthermore, because of the low surface charge density and small size of the primary particles (low  $j_{crit}$ ), limited flocculation occurred in the very early stages of the reaction (<2% conversion).

It was also noted that for the St/Bu system (AA = 0 mol %) a second limited flocculation occurred at a higher conversion (around 58% conversion; see Figure 13). The same behavior has also been reported in a kinetic study of the emulsion polymerization of butadiene (at around 40% conversion) by Weerts and co-workers.<sup>17</sup> They discovered that the reason for this late flocculation (appearing long after the nucleation period, with normal particle size) was the high ionic strength of the aqueous phase, which was caused by changes in the anion concentration during the polymerization, owing to the decomposition of the initiator and adsorption of surface active ions on newly formed surfaces.

For the system with 4 mol % AA, this later limited flocculation did not occur although a decrease in  $N_p$  after ~80% conversion for the 8 mol % AA system can be seen in Figure 13. The latter may have been caused by the formation of highly water-soluble polymers containing carboxylic acid, which resulted in some destabilization of the latex by bridging flocculation.<sup>18</sup> In the 4 mol % AA system, the stability can be attributed to the presence of the carboxyl groups on the surface of the particles. It is well-known that particle stabilization by nonionized carboxyl groups is considered to be by steric stabilization<sup>19</sup> (by either entropic or enthalpic means, depending on the solvent conditions) and that a homogeneous hydrated layer is reported to provide a steric barrier preventing close approach of particles. In this St/Bu/AA latex, the particle surfaces are stabilized by charged surfactant and sulfate end groups, which contribute to the electrical double layer surrounding the particles, and also by uncharged carboxyl groups that form a hydrated water layer. At low electrolyte concentration, the former will extend into the space beyond the polyelectrolyte layer, thereby increasing the repulsive potential energy ( $V_R$ ). However, with increases in the electrolyte concentration and compression of the electrical double layer,  $V_R$  can become small or zero. Under these conditions the particles will still be coated with an extensively hydrated layer of polymeric molecules which provide a steric barrier ( $V_S$ ). Hence, this type of system provides a two-tier mechanism of stabilization against changing ionic strength conditions.

## Conclusions

A model St/Bu/AA emulsion polymerization recipe was carefully selected to approximate industrial application conditions, in addition to being of theoretical interest. The polymerization of this model system resulted in a characteristic S-shape conversion–time curve. The number of particles ( $N_p$ ) increased with increasing conversion during interval I and then rapidly decreased by limited aggregation. At the same time, the surfactant concentration in the aqueous phase dropped to a level below the cmc. Thereafter,  $N_p$  remained almost constant throughout the rest of the reaction. The water-soluble oligomer concentration increased during the nucleation period (interval I), reaching a maximum value, and then started to decrease after  $N_p$  decreased. This may be caused by a stronger interaction between the oligomers and the particle surfaces compared to that between the oligomers and the micelles.

Increasing the AA concentration in the recipe increased the rate of polymerization because of the increased amounts of water-soluble oligomers containing carboxylic acid being initially generated in the aqueous phase, which resulted in the formation of more primary particles during interval I. In the system using 4 mol % AA, no limited aggregation of particles was seen as compared to a parallel reaction without AA. The increased stability was considered to be due to steric stabilization by the carboxyl groups at the particle surface. However, for the 8 mol % AA system, some coagulum and limited aggregation was noted at ~85% conversion, which may have been caused by the formation of high AA content water phase polymer in the later stages of the polymerization leading to bridging flocculation. This will be further discussed in the second paper in this series.

**Acknowledgment.** Financial support from the Emulsion Polymers Liaison Program is gratefully appreciated.

## References and Notes

- (1) Wang, S.; Poehlein, G. W. *J. Appl. Polym. Sci.* **1993**, *49*, 991.
- (2) Kokkeler, C. E. K. The Role of Water-Soluble Oligomers in Emulsion Polymerization. M.S. Report, Lehigh University, 1992.
- (3) Briones, J. A.; Beaton, T. A.; Mullins, J. C.; Thies, M. C. *Fluid Phase Equilib.* **1989**, *53*, 475.
- (4) *Polymer Handbook*, 4th ed.; Brandrup, J., Immergut, E. H., Grulke, E. A., Eds.; Wiley: New York, 1999.
- (5) Odian, G. *Principles of Polymerization*, 3rd ed.; Wiley: New York, 1991; p 340.
- (6) Harkins, W. D. *J. Am. Chem. Soc.* **1947**, *69*, 1428.
- (7) Yeliseyeva, Y. I. In *Emulsion Polymerization*, Piirma, I., Ed.; Academic Press: New York, 1982; p 278.
- (8) Rosen, M. J. *Surfactants and Interfacial Phenomena*, 2nd ed.; Wiley: New York, 1989.
- (9) Maron, S. H.; Elder, M. E.; Ulevitch, I. N. *J. Colloid Sci.* **1954**, *9*, 89.
- (10) Corrin, M. L.; Harkins, W. D. *J. Am. Chem. Soc.* **1947**, *69*, 684.
- (11) Zhao, G. *Physical Chemistry of Surfactants*, 1st ed., University of Beijing: Beijing, 1984; p 244.
- (12) Griffin, W. C. *Offic. Dig. Federation Paint Varnish Production Clubs* **1956**, *28*, 466.
- (13) Godard, E. D. *Colloids Surf.* **1986**, *19*, 255.
- (14) Esuni, K.; Takatu, Y.; Otsuka, H. *Langmuir* **1994**, *10*, 3250.
- (15) Gilbert, R. G. *Emulsion Polymerization: A Mechanistic Approach*; Academic Press: London, 1995; pp 360–455.
- (16) Yuan, X. Y. Ph.D. Dissertation, Lehigh University, 1997.
- (17) Weerts, P. A.; van der Loos, J. L. M.; German, A. L. *Makromol. Chem.* **1990**, *191*, 2615.
- (18) Yuan, X. Y.; Dimonie, V. L.; Sudol, E. D.; El-Aasser, M. S. *J. Appl. Polym. Sci.*, in press.
- (19) Napper, D. H. *Ind. Eng. Chem. Prod. Res. Dev.* **1970**, *9*, 467.

MA020015C